ORIGINAL PAPER

Electrospun composites nanofibers from cellulose acetate/carbon black as efficient adsorbents for heavy and light machine oil from aquatic environment

Nehad A. Elmaghraby[1] · Ahmed M. Omer[2] · El-Refaie Kenawy[3] · Mohamed Gaber[3] · Ahmed El Nemr[1]

Abstract

The feasibility of preparing cellulose acetate/carbon black (CA/CB) composite nanofiber in one step through electrospinning process and investigating its potential oil absorbability and application for machine oil removal from aquatic environment was reported. Different CA/CB composite nanofibers were fabricated by electrospinning of cellulose acetate (CA) solution containing different loads of 0.7, 1.5, and 2.2% CB relative to the weight of CA and labeled as CA/CB0.7, CA/CB1.5, and CA/CB2.2. The scanning electron microscope (SEM) images showed continuous and smooth fiber with submicron diameter ranging from 400–900 nm with good adhering of CB into CA nanofiber. Furthermore, the CA/CB composite nanofibers exhibited high surface area compared with CA nanofiber, which reached 3.057, 2.8718 and 8.244 m^2/g for CA/CB0.7, CA/CB1.5 and CA/CB2.2, respectively. Oil adsorption tests were performed with heavy and light machine oils. The CA/CB composite nanofibers showed higher affinity for oil removal from an aqueous solution than pure CA nanofiber. The CA/CB1.5 composite nanofiber has an exceptional performance for the adsorption of both oils, and the maximum oil adsorbed reached 10.6 and 18.3 g/g for light and heavy machine oils, respectively. The kinetic of machine oils adsorption was fitted well by the pseudo-second-order model. Besides, CA/CB composite nanofiber exposed good adsorption properties and respectable reusability after regeneration for four consecutive cycles. The results advocate the excellent potential of as-fabricated CA/CB composite nanofiber as a promising reusable oil adsorbent for oil spill cleanup applications.

Keywords Cellulose acetate · Carbon black · Composite nanofiber · Oil spill removal · Recyclability

✉ El-Refaie Kenawy
  ekenawy@yahoo.com

✉ Ahmed El Nemr
  ahmedmoustafaelnemr@yahoo.com;
  ahmed.m.elnemr@gmail.com

  Nehad A. Elmaghraby
  nehadaly96@yahoo.com

  Ahmed M. Omer
  ahmedomer_81@yahoo.com

  Mohamed Gaber
  mabuelazm@hotmail.com

[1] Environmental Division, National Institute of Oceanography and Fisheries, El-Anfoushy, Kayet Bey, Alexandria, Egypt

[2] Polymer Materials Research Department, Advanced Technology and New Materials Research Institute (ATNMRI), City of Scientific Research and Technological Applications (SRTA-City), New Borg El-Arab City, P.O. Box: 21934, Alexandria, Egypt

[3] Department of Chemistry, Faculty of Science, University of Tanta, Tanta 31527, Egypt

Introduction

Oil pollution mainly results from offshore oil production, frequent oil spill accidents, marine transportation, petrochemical, and food industries [1–3]. Oil spills may have long-term negative consequences for the ecosystem, affecting marine life survival and human economic activity [4, 5]. Oil was cleaned using traditional methods such as in situ oil burning on water, skimming, ultrasonic separation, mechanical extraction, chemical oxidation, flotation, centrifugation, and gravity separation [1, 6, 7]. Each of these methods has its own limitation [8]. The cleanup technique can be used to separate oil/water-free mixtures in most situations, but it has drawbacks such as poor separation performance, high energy costs, and secondary emissions [9–11]. The latter involves the production of smoke and dust as a result of in situ oil burning on water, as well as contamination by toxic substances as a result of the use of industrial chemical dispersants [1, 12], and they are also ineffective for oil/water

emulsion separation [1, 13]. As a result, oil adsorbents that are both reliable and cost-effective as a mechanical extraction tool are a promising way to deal with oil spills [4].

The synthetic inorganic minerals materials, natural fiber materials, and organic polymers are the three classes that covered the adsorbent materials used in oil spill cleanup [12–16]. The high uptake capacity, hydrophobicity, and oleophilicity, as well as good recoverability, are very important to select the ideal adsorbent material for oil removal [17, 18]. Significant research on natural organic adsorbents has recently been conducted such as the use of Kapok fiber [23, 24], cotton, and rice husks [25], cotton cellulose acetate [26], carbon nanofiber grafted polyurethane [23], cellulose acetate nanofiber membranes [20], raw flax fiber [18], and acrylic acid-grafted pre-plasma nanofibers [25]. Despite the fact that natural organic adsorbents are mostly biodegradable, some of them adsorb both water and oil, reducing separation efficiency, and others can sink during adsorption in harsh sea conditions [26]. Water softening can also be done with a polymeric-clay-magnetite hybrid resin [27] and manufacturing of pH-sensitive PVA/PVP/MWCNT and PVA/PEG/MWCNT nano-composites for application as drug release [28].

On the other hand, synthetic adsorbents designed to combat oil spillages are non-biodegradable man-made materials and they can trigger serious disposal issues after their use [13, 15, 29, 30]. The most famous and widely used synthetic adsorbents for oil removal are polyurethane (PU), polyethylene (PE), and polypropylene (PP) [31]. Chen and Pan [32] and Pavía-Sanders et al. [33] fabricated different oil adsorbent materials having magnetic properties for easy re-pick after the oil adsorption. The β-cyclodextrin oil adsorbents were reusable where the adsorbed oil can be desorbed by a chemical extraction method [34].

Electrospinning is a rare, flexible, and efficient technique for producing nanofiber materials on the sub-micrometer scale, ranging from approximately 50 nm to many micrometers, with fiber diameters ranging from tens of nanometers to micrometers [35, 36]. The electrospun nanofiber mats that result have remarkable properties such as extremely large specific surface areas, porous nanostructures with high degrees of interconnection, and modifiable natures [37]. Because of these properties, electrospun fibers are suitable candidates for applications such as filtration [38], drug delivery [39], chemical and biological protection sensors [40, 41], tissue engineering [42], tissue repair [43], lithium-ion batteries [36] and solar cells [44].

The electrospinning technique is an excellent method for creating unique wet-able surfaces [18, 35, 45]. Recently, a rapid expansion of the nanofibers materials has been fabricated as an effective oil/water separation because fibers can be easily reused, as well as this type of fibers shows a good prospect of application in the treatment of oil pollution [19, 20]. Fiber surface structure, surface adsorption, and capillary voids action all play a role in the oil adsorption process. Esterification is commonly used to increase the hydrophobicity of fibers in order to improve their oil adsorption ability [46]. By simply manipulating a few parameters, solid or internally porous fibers, or a smooth or rough fiber surface, composite mats can be manufactured, and nanoparticles can be incorporated by simply adding the necessary nanoparticles to the polymer solution [13, 15, 47].

Cellulose is one of the world's most plentiful and long-lasting biopolymers, and it can be processed into a valuable cellulose acetate derivative with a wide range of industrial uses [48–50]. Cellulose is inexpensive, biocompatible, and biodegradable, and it has many unique properties such as high strength, light weight, and chemical modification capacity [51, 52]. Cellulose acetate (CA, an acetate ester of cellulose) has been of increasing interest in the past decade in the area of nanofibers [53, 54]. Because of their biocompatibility, biodegradability, and high affinity with other substances, electrospinning of cellulose and its derivatives has received a lot of attention [55]. Since cellulose is difficult to dissolve in traditional solvents, CA is often used as a cellulose substitute [56–59]. It can be used in high-value applications including chromatography [60], fuel cells [61, 62], enzyme bioreactors [63], self-cleaning textiles [64], photochromic devices [65], water treatment [66], and biosensors [67]. Due to its high hydrophobicity, strong solubility in a variety of solvent systems, and low cost, the CA polymer is one of the most commonly used polymers in the preparation of nanofiber membranes [53, 68].

Recently, several attempts have been made to increase electrospun cellulose nanofiber performance for oil treatment. There has been a study on a super hydrophilic graphene oxide-electrospun cellulose composite nanofiber membrane for high-efficiency oil/water separation [69]. The oil/water separation properties of modified cellulose acetate nanofibers with perfluoroalkoxy silanes have been investigated and reported by Arslan et al. [70]. For oil/water separation, a cellulose nanofiber (CNF) aerogel was fabricated and modified by sodium periodate oxidation [71].

Carbon black has attracted much interest since 1990s, practically in the field of chemistry, physics, and materials science. It is a form of elemental carbon that consists of finely particles of carbon produced by incomplete combustion of heavy petroleum products, and it is one of the most stable chemical products [72]. Porous characteristics such as surface area, pore depth, and pore size distribution give it high absorption capacities. In the rubber industry, carbon black (CB) has been used to strengthen rubber to increase its resistance to abrasion, fatigue, tear, and flexing [73]. Many elastomers' tensile strength and processing characteristics are also improved (natural and synthetic) [74].

A new effective eco-friendly cellulose acetate and carbon black (CA/CB) composite nanofiber for the removal of machine oil from water bodies was attempted in this study. In order to allow their exponential advantages to be combined, CA and CB were simultaneously fabricated into one mat via electrospinning technique under optimum preparation conditions. The CA/CB composite nanofiber was characterized using various characterization tools, while its oil adsorption capacity was assayed under different adsorption conditions. Moreover, kinetics of the oil adsorption process and the aptitude of the developed composite nanofiber to reuse were also explored.

Materials and methods

Materials

CA (acetyl content: 29–46%, Mn: 50,000) was purchased from ALPHA Chemie, India. N-Hexane 95% from M-TEDIA. Carbon black (mesoporous of 10 ± 1 nm average pore diameter, BET surface area of 150 m^2/g, and particle size of 45 ± 5 μm) from ASMA dye, Egypt. Polyethylene glycol (PEG) from ACROS Organic (Mwt = 200). Acetone for HPLC grade from Central Drug House, assay 99.8%. N,N-dimethylacetamide (DMAA) from Merck. Ethyl alcohol from International Company for sup & MED, Industries, Egypt. Exxon Mobil, Egypt (Fully Synthetic Motor Oil 5 W-50, Rally formula) provided heavy (Viscosity 32 cSt at 40 °C) and light machine oil (Viscosity 5.5 cSt at 40 °C), and all chemicals were used without further purification.

Preparation of CA/CB solution

CA (12 percent w/v) was dissolved in a DMAA/acetone binary solvent mixture (4:1 v/v) to produce homogeneous solutions. PEG was used to help the electrospinning process resolve the surface tension of the solution. (The ratio of PEG/CA was 1:1 w/w.) Three different concentrations of carbon black (CB) were added to CA solution (0.7, 1.5 and 2.2 w % of CA) to obtain CA/CB composite electrospun. Further increase of the CB percentage led to precipitate of the excess CB and close the needle. Complete polymer dissolution in the co-solvent was prepared by continuously stirring at room temperature for 2 h in 500 mL conical flasks, and then, polymer solutions were ultrasonicated overnight at room temperature. After mixing, the polymer solutions were left undisturbed for a day to facilitate the release of air bubbles in the solution [75].

Electrospinning of CA/CB solutions

Using a 20 mL syringe fitted with a blunt-ended metal needle, electrospinning was performed in horizontal orientation at an applied voltage of + 26 kV and –10 kV using a Bioinicia, FLUIDNATEK LE-50 electrospinning unit. The temperature was 24 °C, and humidity was less than 20% [76, 77]. The composite polymer solution was subjected to electrospin using a 20-mL syringe pump operating at 10 mL/h and 10 cm distance far from the collector. Webs were collected on cylinder aluminum collector with rotation speed of 500 rpm. The electrospun samples were removed from the collector and washed with ethanol to complete removal of PEG and then dried in a vacuum oven at 50 °C for 24 h and labeled as CA/CB0.7, CA/CB1.5, and CA/CB2.2 [78]. The electrospin was continued for 10 h for each concentration.

Characterization of the electrospun CA/CB composites nanofibers mats

FTIR spectroscopy of the samples was conducted in the wave number range from 400 to 4000 cm^{-1} by using Bruker VERTEX70 connected to platinum ATR unit (model V-100), Germany. Surface area and pore size distribution of fabricated CA/CB composite nanofibers were carried out by nitrogen adsorption–desorption isotherms measured at 77 K using BELsorp mini II, BEL Japan, Inc., Japan. The Brunauer–Emmett–Teller (BET) equation was used to measure the real surface area from the N$_2$ adsorption isotherm, and the single point total pore volume was determined from the nitrogen sum adsorbed at 0.95 relative pressure. A scanning electron microscope (SEM) was used to investigate the morphology and scale of the samples (JEOL, Model JSM 6360LA, Japan). Sample was coated by a gold thin layer for SEM analysis. An Image-G program was used to calculate the average fiber diameter (AFD) of the electrospun fibers. Thermogravimetric analysis (TGA) of the fabricated CA/CB nanofiber was analyzed by SDT 650 Simultaneous Thermal Analyzer, the USA. Each powdered sample was heated by 10 °C/min. Up to 900 °C, about 15 mg of each samples was taken in silica crucible and subjected to pyrolysis under N$_2$ flow [79].

Water uptake capacity

The ability of CA/CB composite nanofiber mats to adsorb water was investigated in order to better understand how water molecules diffuse into the nanofiber mats, which is critical for oil removal. The nanofiber mats (0.6 g; fiber shape) were immersed directly in certain amount of three water medium of pH values 3, 6 and 11 at room temperature for 24 h, and then, the samples were taken out and dried gently with filter paper to remove the excess water and

subsequently weighed to define weight of swollen nanofiber (Ws) and after the swollen product was dried at 50 °C to a constant weight (weight of dried nanofiber, Wd). Following Eq. (1) is used to measure the percentage of swelling ratio of the sample [80].

$$Swelling\ ratio\% = \frac{Ws - Wd}{Wd} \times 100 \tag{1}$$

Determination of oil adsorption capacity and retention capacity (static test)

The oil adsorption ability and retention were calculated using the standard procedure defined in ASTM 726–06, "Standard Test Method for Absorbent Performance of Adsorbents." The fibers (0.5 g in mass) of CA/CB0.7, CA/CB1.5, and CA/CB2.2 composites nanofibers were placed into 250 mL glass beaker for 1 h, and the samples were weighed and then slowly immersed in 30 mL oil (heavy or light machine oils) at room temperature (24±2 °C). After soaking for the desired time, the samples were taken out and left to drain for 5 min followed by lifted for 24 h through a wire mesh to remove any loosely attached liquid and free oil dripping out then weighed for each time. All of the tests were repeated three times, with the average value used to determine the final results. The oil uptake capacity of the samples was also carried out to measure the amount of heavy or light machine oil taken by the samples. The oil adsorption capacity (Q) and retention capacity are calculated according to Eqs. (2) and (3) [22, 81].

$$Oil\ sorption\ capacity(Q) = \frac{W_5 - W_i}{W_i} \tag{2}$$

$$Oil\ retention\ capacity = \frac{W_{24} - W_i}{W_5 - W_i} \tag{3}$$

where W_i is the initial mass of sample before adsorption (g), W_5 is the mass of oil wetted sample at 5 mind ripping (g), and W_{24} is the mass of oil wetted sample at 24 h dripping (g).

Adsorption capacity determination (oil/water solution) (Dynamic test)

The adsorption test was carried out using light and heavy machine oils as model oils, with the aim of determining if structured fiber could be used to selectively absorb spilled oil from water surfaces [22, 81, 82]. Machine oil (30 mL) was poured over 50 mL of seawater, and then, 0.4 g structured fiber was put in the 250 mL jar containing the oil sample and the seawater was mounted in a shaker at 200 rpm. The samples were taken out at various intervals (5, 10, 15, 30, and 60 min), then raised and put on a wire mesh with

free oil dripping out for 5 min before being weighted. The samples were then moved to the piston, where the adsorbent was pressed five times through the press to remove the oil. A small amount of n-hexane was applied to the press during the pressing stage to aid in the extraction of the oil. By using the centrifuge technique defined in ASTM D1696-91, the liquid was collected in a graduated centrifuge tube for water content determination [83]. Each sample was tested for 3 times, and only the mean values were reported. The oil adsorption capacity (g/g) is calculated according to Eq. (4).

$$Oil\ sorption\ capacity = \frac{(W_S - W_W) - W_i}{W_i} \tag{4}$$

where W_S is the weight of saturated adsorbent (water + oil + adsorbent), W_W is the weight of adsorbed water, and W_i is the initial dry weight of adsorbent [84].

Kinetics studies

The experimental data were further analyzed using a pseudo-first-order model and a pseudo-second-order model, as expressed in linear forms in Eqs. (5) and (6), respectively, to better understand the adsorption mechanism [19, 20, 85–87]:

$$\log (q_e - q_t) = \log q_e - \frac{K_1}{2.303}t \tag{5}$$

$$\frac{t}{q_t} = \frac{1}{K_2 \times q_e^2} + \frac{t}{q_e} \tag{6}$$

where q_t (g/g) and q_e (g/g) are the amount of oil adsorbed at time t (min) and equilibrium, respectively, and K_1 and K_2 are the adsorption rate constants.

Reusability test

From an economic standpoint, reusability is one of the most important considerations to consider when choosing products. At room temperature, 0.5 g of dried CA/CB composite nanofiber samples were immersed in 30 mL oil for 1 h. The samples were then drained for 5 min until the wet sample was weighed. Finally, the oil was removed from the oil-saturated samples by centrifugation, followed by washing with 3 mL hexane and centrifugation four times. After 10 min, the samples were put in a 60 °C oven for 24 h before being reused. The process was replicated in a water/oil system with 0.4 g of fiber in 50 mL seawater and 30 mL oil for 15 min for heavy machine oil and 1 h for light machine oil, and the oil adsorption capacity of the sample was measured after each cycle as described above.

Result and discussion

Characterization of cellulose/carbon black composites nanofibers

Scanning electron microscope

The morphologies and fiber diameter distribution of CA, CA/CB0.7, CA/CB1.5, and CA/CB2.2 composites nanofibers are exhibited in Fig. 1. The morphology structure was bead-free cylindrical and smooth fibers with submicron diameters. Fiber diameter of the composites nanofibers increases with increasing of CB content. AFD for CA, CA/CB0.7, CA/CB1.5, and CA/CB2.2 were 495, 628, 727, and 831 nm, respectively, as calculated as an average value from 20 measurements using ImageJ software. It was

obvious that very few CB particles were adhered to the surface of the fibers. This finding revealed that the presence of a small amount of carbon black has a minor impact on nanofiber diameter. When a small amount of carbon black is added to cellulose acetate nanofiber, the diameter of the nanofiber increases. Surprisingly, SEM research revealed that the surface of nanofibers appeared dense and relatively homogeneous tiny particles, indicating that CB adhered to the surface. There are also several pores on the fiber's surface, which resulted from the removal of PEG from the surface. [88] (Chen et al. 2009).

FTIR spectra

Figure 2 shows the FTIR spectra of CA, CB and the CA/CB0.7, CA/CB1.5, and CA/CB2.2 composites nanofibers. Cellulose acetate and composite samples exhibited same

Fig. 1 Images of SEM for **a** CA nanofiber, **b** CA/CB1.5 composite nanofiber, **c** CA/CB0.7 composite nanofiber, **d** CA/CB2.2 composite nanofiber and **e** surface morphology of the distribution of CB into CA nanofiber for CA/CB2.2 using 15 kV and 5000X magnification
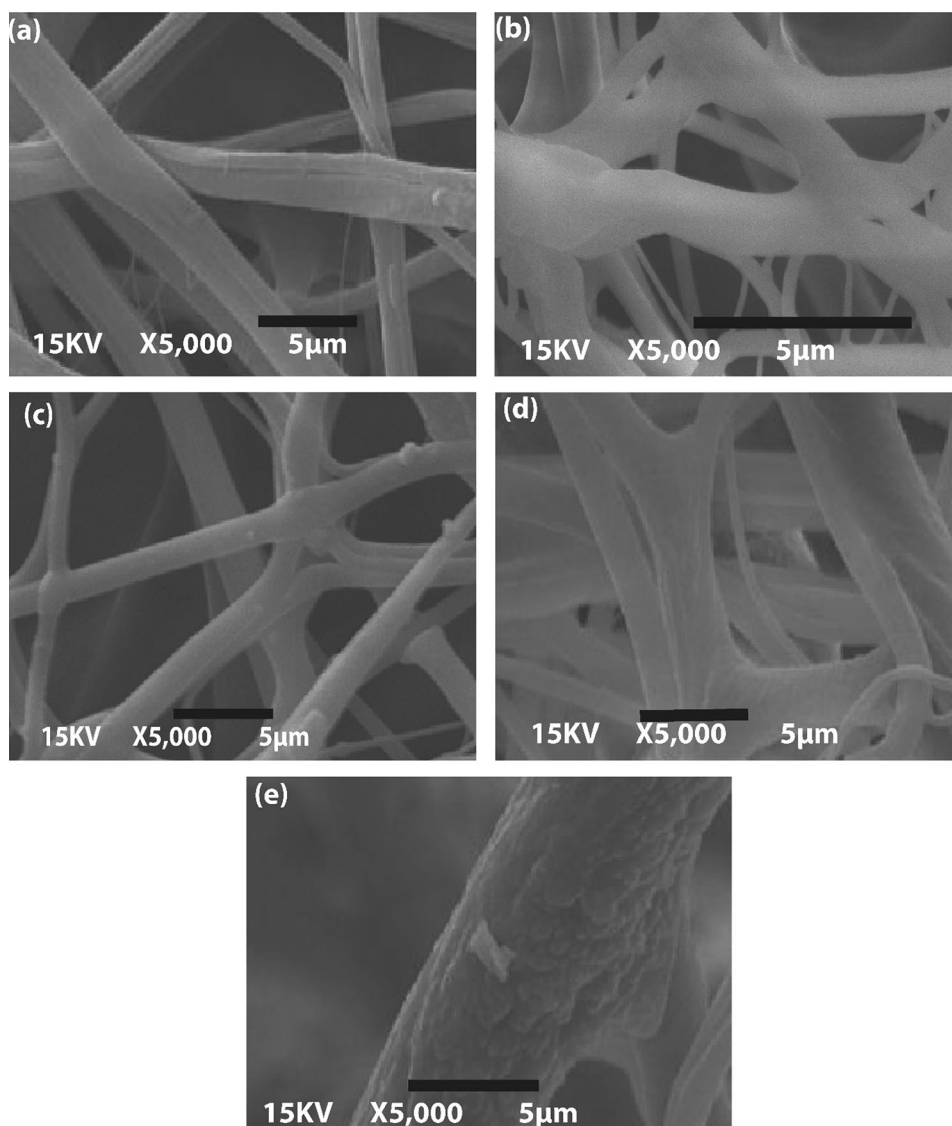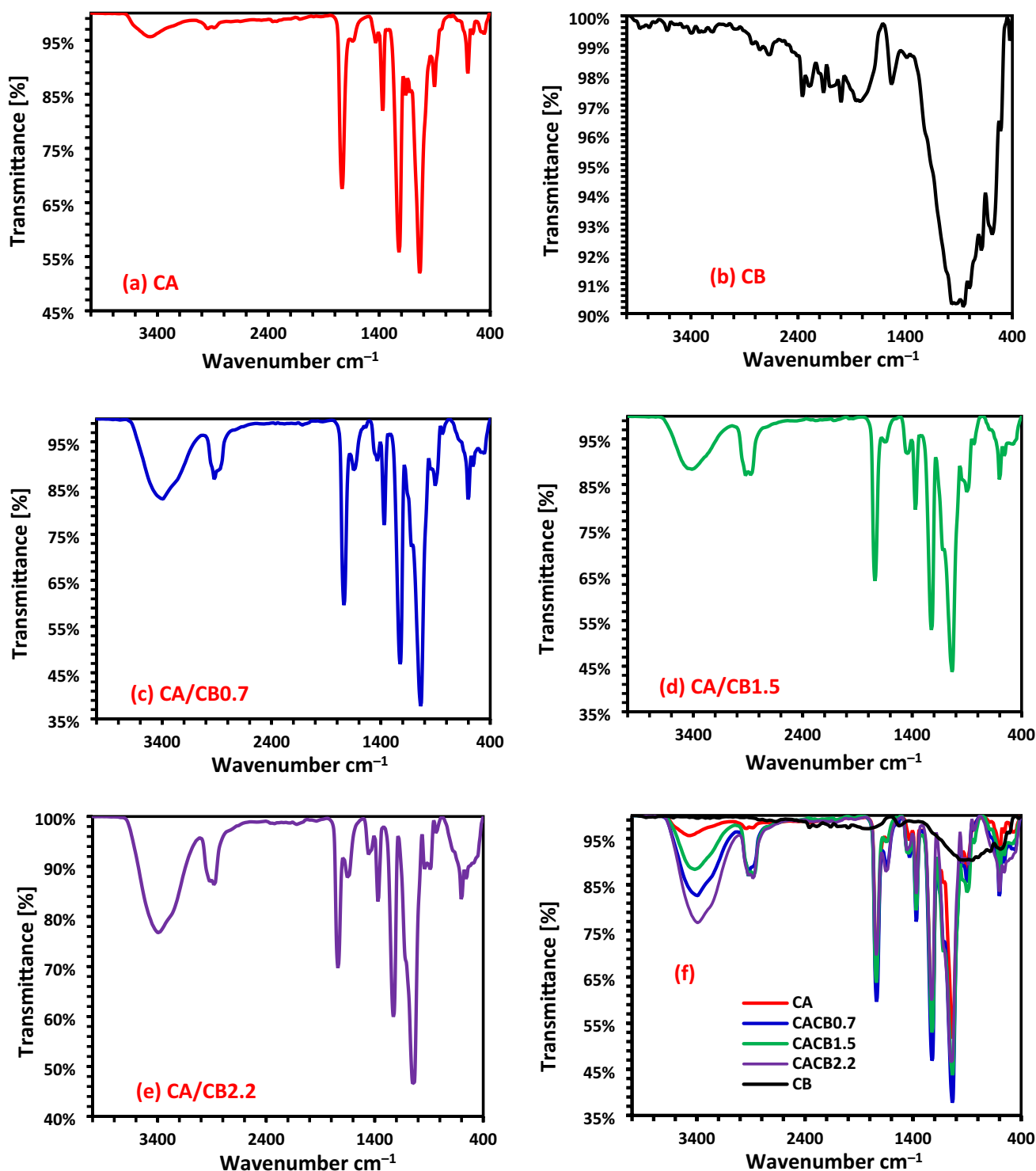
Fig. 2 FTIR spectra of **a** CA;, **b** CB, **c** CA/CB0.7, **d** CA/CB1.5, **e** CA/CB2.2, **f** a-e in one plot

peaks as broad band around 3394 cm^{-1} assigned to O–H stretching vibration and small peak at 2943 cm^{-1} assigned for C-H stretching vibration in CA was highly increased in the composite nanofiber samples and appeared as two peaks at 2921.4 and 2872.6 cm^{-1} due to the presence of CB in the three composites. The adsorption peak at 1737 cm^{-1} originates from C=O stretching vibration of ester [89]. C-O and C-H bending vibrations are responsible for the bands around 1228 and 1368 cm^{-1}, respectively. C-O stretching in cellulose acetate was given a wide band at 1050 cm^{-1}. The FTIR

spectra of CB exhibited three peaks at 850 cm^{-1} assigned to (C–C) carbon skeleton, 1530 cm^{-1} assigned to stretching (C–C) and 2395 cm^{-1} originate from CO_2. By comparison FTIR spectra of CA/CB composite fibrous with that of pure CA fibrous, there is no change on the peaks.

Surface area analysis

Adsorption–desorption plot of CA, CB, CA/CB0.7, CA/CB1.5, and CA/CB-2.2 is shown in Fig. 3. All samples belong to type V isotherms corresponding to IUPAC classification indicating that they are low energy, homogeneous solid surface possessing mesoporosity [90, 91]. It can be achieved using mesoporous or microporous adsorbents with weak adsorbent–adsorbate interactions. Besides, isothermal loop deceleration does not stabilize at relative pressures near saturation vapor pressure, indicating that mats contain slit-like pores. The hysteresis loop was brought about the capillary condensation in the mesoporous nanofiber. Since the surface properties of the adsorbents are important, BET measurements were used to calculate the surface area,

Table 1 Surface area, total pore volume and mean pore diameter of composite samples

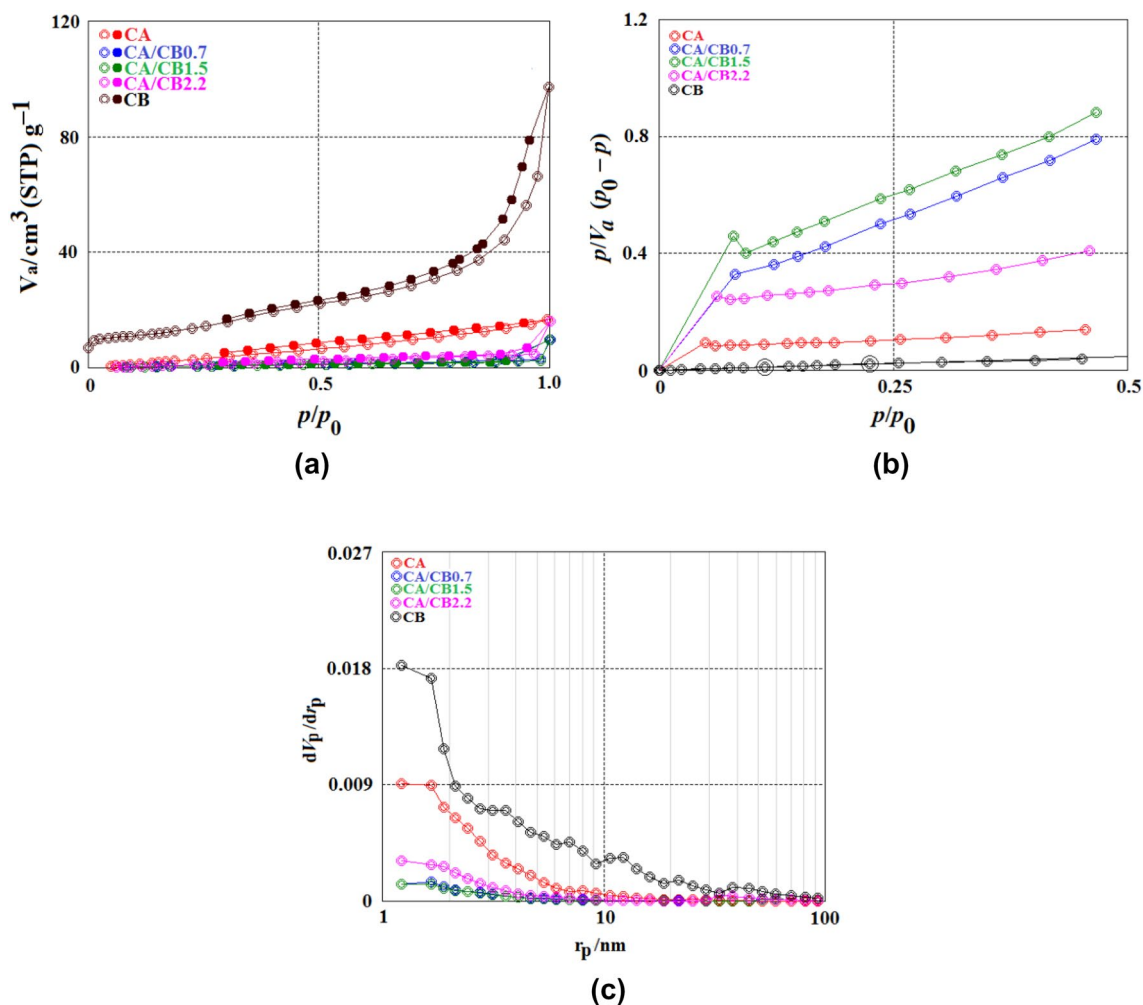| Sample code	S_{BET} (m^2/g)	V_m (cm^3/g)	M_p (nm)	S_{mi} (m^2/g)	V_{mi} (cm^3/g)
CB	47.422	0.1339	11.297	52.011	0.1328
CA	25.593	0.0253	3.961	23.115	0.0301
CA/CB0.7	3.0571	0.0094	12.307	3.596	0.0099
CA/CB1.5	2.8718	0.0086	12.516	3.3795	0.0095
CA/CB2.2	8.244	0.0178	9.1128	7.919	0.0204

Fig. 3 **a** N$_2$ gas adsorption – desorption isotherms. **b** BET analysis, and **c** BJH analysis of CA, CB, CA/CB0.7, CA/CB1.5, and CA/CB2.2 nanofiber composite

average pore diameter, and pore volume of the CA and CA/CB composites nanofibers, and the results are shown in Table 1.

The surface area of the CA was noticed to be slightly decreased with increasing CB content in the composite nanofiber up to 1.5% and then further increasing CB content up to with 2.2% CB. These observations could be ascribed to the surface irregularities of the CA/CB. The specific surface area values of CA and CB were 25.593 and 47.422 m^2/g, respectively. Besides, the specific surface area of CA nanofiber was found to be higher than that reported by Goetz et al. [92] as 2.73 m^2/g for CA nanofiber. The specific surface area (S_{BET}) values of CA/CB0.7, CA/CB1.5 and CA/CB2.2 composites nanofibers were 3.057, 2.8718 and 8.244 m^2/g, respectively. The mean pore diameters (M_p) of 10.638, 12.307, 12.516, and 9.1128 nm were determined for CA/CB0.7, CA/CB1.5 and CA/CB2.2 composites nanofiber mats, respectively (Fig. 3). Meanwhile, the maximum micropore surface area (S_{mi}) and micropore volume (V_{mi}) of CB, CA, CA/CB0.7, CA/CB1.5 and CA/CB2.2 nanofiber mats were 52.011, 23.115, 3.596, 3.3795, 7.919 m^2/g and 0.1328, 0.0301, 0.0099, 0.0095, and 0.0204 cm^3/g, respectively. These results showed that the surface area and pore volume were dramatically decreased by addition of carbon black to the cellulose acetate.

Thermogravimetric analysis (TGA)

TGA in a nitrogen atmosphere was used to assess the thermal stability of the electrospun fibers. Figure 4 shows the TGA curves of pure CA nanofiber, and CA/CB nanofiber composites with different CB loadings. All samples fiber mat exhibited two steps thermal transitions, with the low-temperature(i.e., 50–150 °C) gave weight losses 10.32, 10.97, 12.31, and 13.76% for CA, CA/CB0.7, CA/CB1.5,

and CA/CB2.2, respectively, corresponding to the loss of moisture, while at higher-temperature (i.e., 350 –400 °C) gave weight losses 73.01, 77.7, 75.47, and 74.69% for CA, CA/CB0.7, CA/CB1.5 and CA/CB2.2, respectively. In addition, the residues of samples after thermal decomposition at 900 °C were 16.67, 11.34, 12.21, 11.56%, and 16.67% for CA, CA/CB0.7, CA/CB1.5, and CA/CB2.2, respectively.

Differential scanning calorimetry (DSC) analysis is used to have specific information onto thermal transitions state [93, 94]. Via monitoring the heat flow over temperatures, it offers insight into a material's phase changes (melting point, boiling point, and fusion), glass transition temperatures (Tg), and the heat capacity (Cp). DSC analysis of pure CA nanofiber and CA/CB composites nanofibers with different CB loadings is shown in Fig. 4b. All samples exhibited a endopeak represented a temperatures at 61.07, 84.82, 85.99 and 78.74 °C for CA, CA/CB0.7, CA/CB1.5 and CA/CB2.2, respectively, that are attributed to water loss from the sample. Similarly, the melting peak represented a degradation temperatures was 575.17, 609.65, 478.65 and 453.89 °C for CA, CA/CB0.7, CA/CB1.5 and CA/CB2.2, respectively [54, 95].

Swelling behavior

The swelling activity of the pure CA and composite CA/CB fibrous mats was investigated further (Fig. 5). The swelling properties of CA and CA/CB composites were studied in media of different pH values (3, 6 and 11) for 24 h. The maximum swelling ratio of pure CA mat was 130.4% at pH 6, and all of the CA/CB composite fiber mats exhibited higher values of swelling at the same pH for CA/CB0.7 (166.1%), CA/CB1.5 (188.9%) and CA/CB2.2 (153.3%). As a result, the swelling ratio was lowest in pH 3 and significantly higher in neutral and alkaline environments. The alkaline
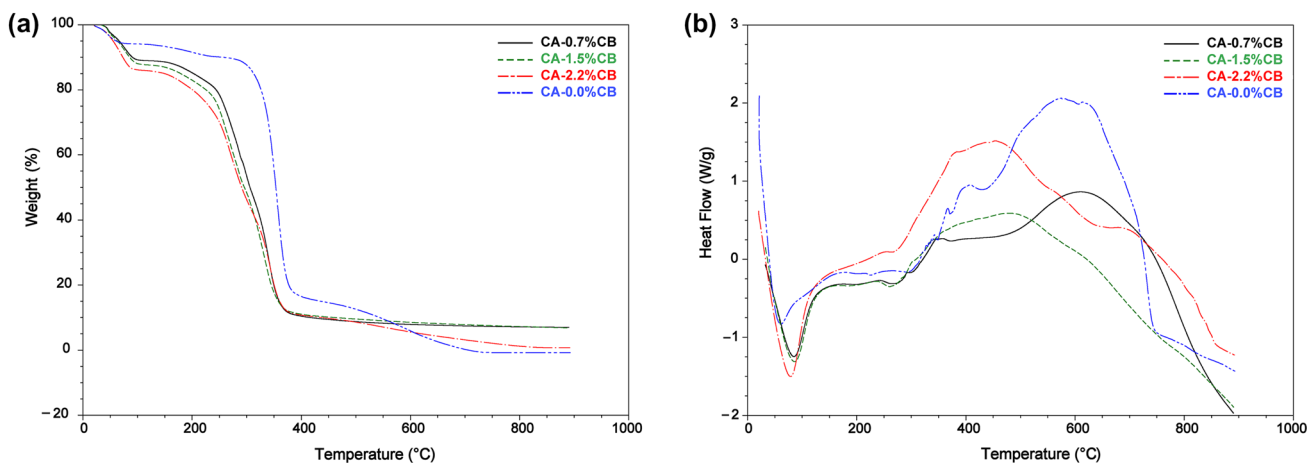

Fig. 4 (**a**) TGA, **b** DSC curves of the CA, CA/CB0.7, CA/CB1.5, and CA/CB2.2 composites nanofibers at temperature ranged between 50 and 900 °C under flow of N_2 (100 mL/min)
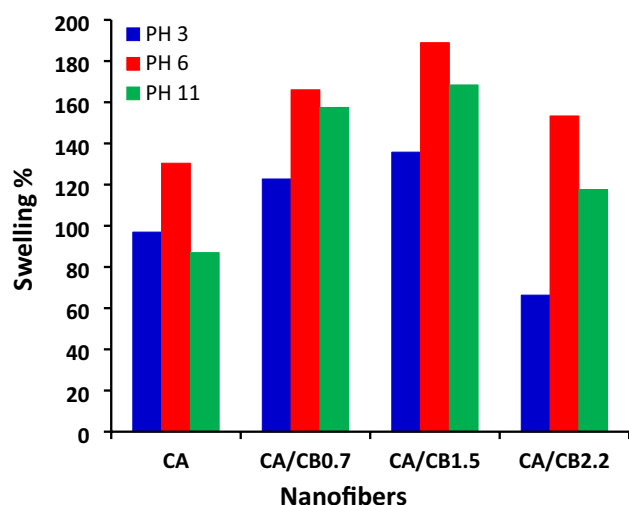
Fig. 5 Swelling equilibrium behaviors of the CA, CA/CB0.7, CA/CB1.5, and CA/CB2.2 composites nanofibers at pH 3, 6, and 11 at room temperature

condition obviously increased swelling, whereas the acidic condition decreased swelling, and this finding is consistent with that reported in the literature [96, 97]. The swelling ratio of CA/CB composite nanofiber was higher than that of native CA nanofiber. This is because the presence of CB increases the inter-spaces between the CA chains, which improves the penetration of water molecules into the nanofiber network, and as a result, the swelling ratio rises [80]. However, increasing the amount of CB to 2.2% in the composite reduced the swelling that might be attributed to the possibility that excess CB might block pores in the fiber network and thus reduce water adsorption.

Oil adsorption and retention capacity

Oil adsorption and retention capability are two critical properties of an adsorbent used to recover spilled oils [1]. Table 2 lists the oil adsorption and retention capacity values for the fabricated composites. In general, heavy machine oil adsorbs significantly more than light machine oil. This may be explained by the fact that heavy machine oil is viscous in comparison to light machine oil in the same unit volume.

Basically, the high viscosity can improve the oil adsorption process through boosting the adhered oil molecules on the adsorbent surface [61, 62]. On the other hand, light machine oil was more ready to drip out from the stain steel mesh than heavy machine oil [22, 98]. The synthetic fibers demonstrated high oil adsorption and retention capabilities which adsorbed more than 12 times the mass of oils over their own weight and retained more than 76% of the oil adsorbed after 24 h of dripping. Furthermore, CA nanofibers with different CB contents showed a high oil capacity than neat CA nanofiber. The results referred that CA fiber with 2.2% CB (CA/CB2.2) was preferable to obtain higher oil adsorption performance, and however, more oil retention was observed for CA fiber with 1.5% CB (CA/CB1.5). Introducing more amounts of CB to the composite nanofibers may reduce the ability of the composite nanofibers to retain oil molecules in the fibers [32, 99].

Batch adsorption experiments

Batch adsorption experiments in oil/water mixtures were used to determine the maximum oil adsorption capacities of CA/CB0.7, CA/CB1.5, and CA/CB2.2 for machine oil. The results clarified that CA/CB0.7, CA/CB1.5 and CA/CB2.2 exhibited fast adsorption rate during the initial 5 min in case of heavy and light machine oil (Fig. 6). Moreover, the maximum oil adsorption capacity for heavy and light machine oils was recorded after 15 min as 18.37 and 10.621 g/g, respectively, using CA/CB1.5 composite nanofibers. The oil adsorption potential increases marginally within the first 15 min of contact time, and then, the adsorption process becomes relatively sluggish for all adsorbents, which can be due to the fact that the oil on the outside of the fibers slowly penetrates into the adsorbent material's hollow cavity. This observation is consistent with the findings reported by Thompson et al. [100] and Wang et al. [19, 20].

Kinetics studies

The kinetics of oil adsorption defines the rate of oil absorption by fiber; this rate determines the operation, and it is necessary to determine the optimum operating conditions. The kinetic parameters provide critical information for designing
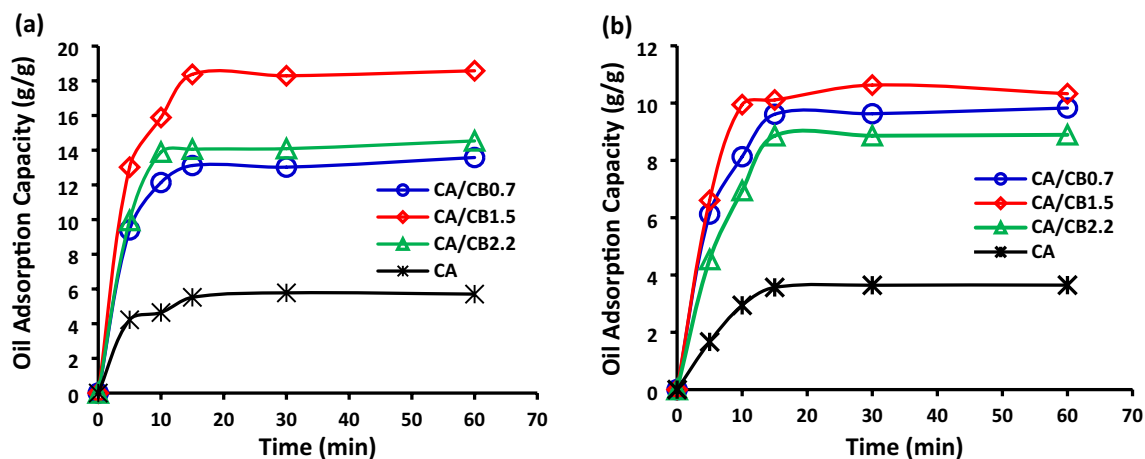
Table 2 Oil capacity and oil retention of heavy and light machine oil in 20 mL oil with 0.5 g of CA nanofiber and CA/CB composites nanofibers for 1 h (dynamic test)

Sample code	Heavy machine oil		Light machine oil	
	Oil adsorption capacity (g/g)	Oil retention capacity (%)	Oil adsorption capacity (g/g)	Oil retention capacity (%)
CA	5.89	76	4.45	80
CA/CB0.7	12.31	76	10.62	82
CA/CB1.5	12.56	84	12.01	83
CA/CB2.2	12.73	72	12.95	81

Fig. 6 Oil adsorption capacity of **a** heavy machine oil, **b** light machine oil (5 mm of oil thickness on 400 mg of adsorbent) at room temperature
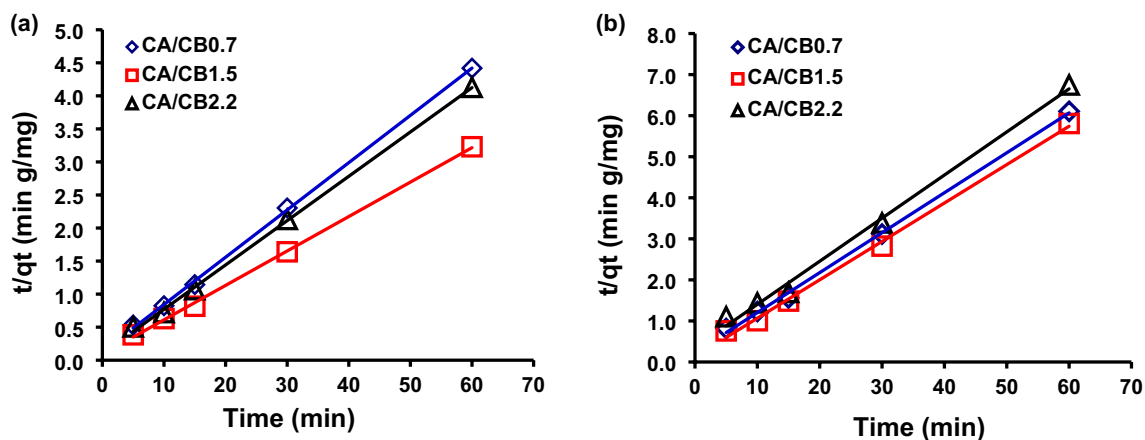

Fig. 7 The Plot t/q_t versus t of the pseudo-second-order model for removal of **a** heavy machine oil, **b** light machine oil (5 mm oil thickness) by CA/CB composites nanofibers at room temperature

Table 3 The first- and second-order adsorption rate constants, as well as measured and experimental q_e values for heavy and light machine oils, were compared using CA/CB composite nanofibers

Parameter			First-order kinetic model			Second-order kinetic model			
Sample	Machine Oil	q_e(exp.)	$k_1 \times 10^3$	q_e(calc.)	R^2	$k_2 \times 10^3$	q_e(calc.)	h	R^2
CA/CB0.7	Heavy	13.11	117.22	122.18	0.455	40.37	13.97	7.88	0.999
CA/CB1.5		18.37	167.66	1948.04	0.455	30.36	19.19	11.18	0.999
CA/CB2.2		14.05	114.46	88.23	0.34	45.20	14.90	10.04	0.999
CA/CB0.7	Light	9.061	14.74	1.98	0.369	41.09	10.28	4.34	0.998
CA/CB1.5		10.11	-0.69	1.00	0.0003	66.79	10.70	7.64	0.997
CA/CB2.2		8.89	18.65	2.39	0.414	13.21	9.52	2.83	0.994

and modeling oil adsorption processes. As a result, the kinetics of oil adsorption on the prepared fiber were investigated using pseudo-first-order (Eq. 5) and pseudo-second-order (Eq. 6) kinetic models. The value of the correlation coefficients expresses the applicability of a kinetic model (R^2, values close or equal to 1). The model with the higher value

is more applicable to the kinetics of oil adsorption. The pseudo-second-order kinetics model was expressed via plot of t/q_t versus t, where k_2 and q_e obtained from the intercept and slope of the plot (Fig. 7). The linear plots of t/q_t versus t show good agreement between experimental and calculated q_e values for different samples for heavy and light machine

oils (Table. 3). The R^2 values for the pseudo-second-order kinetic model are > 0.994. Based on these findings, it is assumed that the pseudo-second-order kinetic model, as opposed to the pseudo-first-order kinetic model, offered a better correlation for oil adsorption onto fiber.

Reusability

The material's reusability is also an effective indicator for removing unintentionally spilled oil. Using *n*-hexane extraction, the oil-saturated samples were recycled for multiple adsorption/desorption cycles. The centrifuge method of recovering oil from adsorbent material is both cost-effective and practical. As a result, the recovery of the oil from the adsorbent material, as well as the feasibility of reusing the adsorbents, was investigated. The changes in oil adsorption capacity of CA/CB0.7, CA/CB1.5, and CA/CB2.2 for oil/water system are displayed in Fig. 8 and Table. 4 for static oil adsorption indicated that the fibers show higher oil uptake in the first cycle, and then, its adsorption capacity decreased and remain constant in the other cycles. Teli and Valia [101] reported that hexane extraction did not considerably affect

the stability and chemical composition of the fibers. The findings suggest that the CA/CB composite nanofibers can be reused and recycled several times using the centrifuge process. As a result, they are highly promising oil-absorbing materials for oil spill cleanup.

Conclusion

The current study found that cellulose acetate/carbon black composite nanofibers absorbed more oil than pure cellulose acetate in oil and oil/water mixtures. The chemical compositions, surface morphology, and thermal stability of the formed composite nanofibers were investigated using FTIR, SEM, and thermal analysis tools. A pseudo-second-order model can be used to suit the relevant kinetics data. This indicated that CA and CB had synergetic effect. In addition, the CA/CB composites nanofibers showed a good oil-absorption capacity with a decent reusability for 4 repeated cycles. Based on these findings, there is no question that the adapted fibers can be used as a promising replacement for traditional oil adsorbents in the cleanup of oil spills in
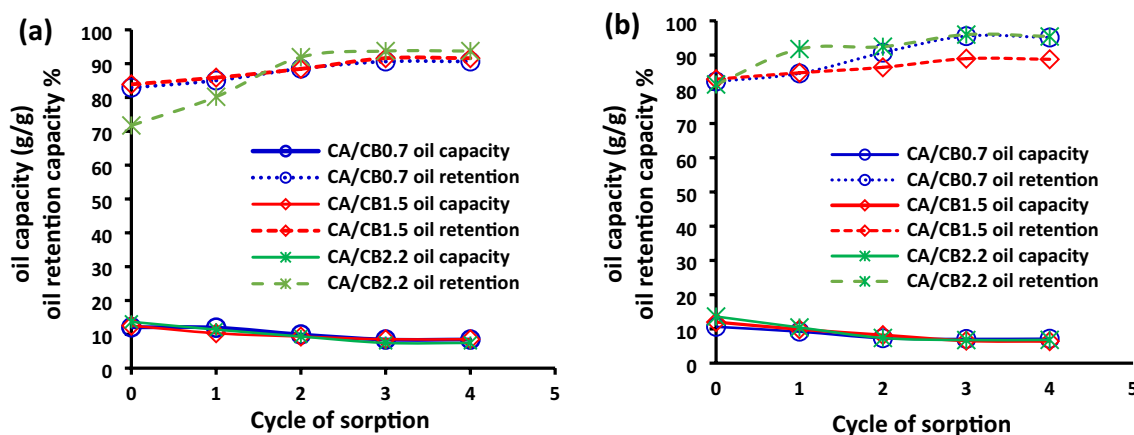

Fig. 8 The reusability (oil capacity and oil retention) of CA/CB composites nanofibers for **a** heavy machine oil/water, **b** light machine oil system for 4 cycles

Table 4 The reusability of CA/CB composites nanofibers for dynamic oil (4 cycles) for heavy and light machine oils

Cycles	Heavy machine oil						Light machine oil					
	CA/CB0.7		CA/CB1.5		CA/CB2.2		CA/CB0.7		CA/CB1.5		CA/CB2.2	
	OC	OR	OC	OR	OC	OR	OC	OR	OC	OR	OC	OR
0	12.09	82.92	12.56	83.89	13.70	71.73	10.62	82.27	12.01	82.95	13.62	81.40
1	11.97	85.02	10.33	85.87	11.40	80.20	9.20	84.63	9.89	84.82	10.43	91.75
2	9.95	88.52	9.35	88.45	9.36	91.92	7.29	90.70	8.20	86.41	7.36	92.44
3	8.47	90.63	8.54	91.61	7.47	93.72	7.08	95.52	6.57	88.94	6.75	95.98
4	8.47	90.63	8.54	91.61	7.47	93.72	7.14	95.12	6.41	88.76	6.81	95.42

OC oil capacity (g/g); *OR* oil retention (%)

aqueous environments. The maximum oil adsorption capacity was reported for the nanofiber labeled as CA/CB2.2, while the maximum oil retention capacity was reported for the nanofiber labeled as CA/CB1.5 for both heavy and light machine oil.

Data availability The datasets analyzed during the study are available from the corresponding author on request.

Declarations

Conflict of interest The authors declare that they have no conflict of interest.

References

1. A. El Nemr, Petroleum contamination in warm and cold marine environment. Nova Science Publishers, Inc. Hauppauge New York. [ISBN 1–59454–615–0] (2005) 150pp

2. A. El Nemr, From natural to synthetic fibers. in Book entitled: Textiles: Types, Uses and Production Methods, A. El Nemr (eds). Nova Science Publishers, Inc. Hauppauge New York. (2012) pp. 1–152. ISBN**:** 978–1–62100–239–0

3. Z. Wang, J.P. Barford, C.W. Hui, G. McKay, Kinetic and equilibrium studies of hydrophilic and hydrophobic rice husk cellulosic fibers used as oil spill sorbents. Chem. Eng. J. **281**, 961–969 (2015). https://doi.org/10.1016/j.cej.2015.07.002

4. F. Aguilera, J. Méndez, E. Pásaroa, B. Laffona, Review on the effects of exposure to spilled oils on human health. J. Appl. Toxicol. **30**(4), 291–301 (2010). https://doi.org/10.1002/jat.1521

5. A. El Nemr, Impact, monitoring and management of environmental pollution. Nova Science Publishers, Inc. Hauppauge New York. [ISBN-10: 1608764877, ISBN-13: 9781608764877]. (2011) 638 pages

6. A. Tanvir, V.P. Ting, S.J. Eichhorn, Nanoporous electrospun cellulose acetate butyrate nanofibres for oil sorption. Mater. Lett. **261**, 127116 (2020). https://doi.org/10.1016/j.matlet.2019.127116

7. G. Akhlamadi, E.K. Goharshadi, Sustainable and superhydrophobic cellulose nanocrystal-based aerogel derived from waste tissue paper as a sorbent for efficient oil/water separation. Process Saf. Environ. Prot. **154**, 155–167 (2021). https://doi.org/10.1016/j.psep.2021.08.009

8. Z. Jiang, L.D. Tijing, A. Amarjargal, C.H. Park, K.-J. An, H.K. Shon, C.S. Kim, Removal of oil from water using magnetic bicomponent composite nanofibers fabricated by electrospinning. Compos. B **77**, 311–318 (2015). https://doi.org/10.1016/j.compositesb.2015.03.067

9. A. Jamsaz, E.K. Goharshadi, An environmentally friendly superhydrophobic modified polyurethane sponge by seashell for the efficient oil/water separation. Process Saf. Environ. Prot. **139**, 297–304 (2020). https://doi.org/10.1016/j.psep.2020.04.042

10. A. Jamsaz, E.K. Goharshadi, Flame retardant, superhydrophobic, and superoleophilic reduced graphene oxide/orthoaminophenol polyurethane sponge for efficient oil/ water separation. J. Mol. Liq. **307**, 112979 (2020). https://doi.org/10.1016/j.molliq.2020.112979

11. A. Jamsaz, E.K. Goharshadi, A. Barras, M. Ifires, S. Szunerits, R. Boukherroub, Magnetically driven superhydrophobic/superoleophilic graphene-based polyurethane sponge for highly efficient oil/water separation and demulsification. Sep. Purif. Technol. **274**, 118931 (2021). https://doi.org/10.1016/j.seppur.2021.118931

12. G. Coelho, J. Clark, D. Aurand, Toxicity testing of dispersed oil requires adherence to standardized protocols to assess potential real world effects. Environ. Pollut. **177**, 185–188 (2013). https://doi.org/10.1016/j.envpol.2013.02.004

13. X. Wang, J. Yu, G. Sun, B. Ding, Electrospun nanofibrous materials: a versatile medium for effective oil/water separation. Mater. Today **19**(7), 403–414 (2016). https://doi.org/10.1016/j.mattod.2015.11.010

14. M. Chhajed, C. Yadav, A.K. Agrawal, P.K. Maji, Esterified superhydrophobic nanofibrillated cellulose based aerogel for oil spill treatment. Carbohydr. Polym. **226**, 115286 (2019). https://doi.org/10.1016/j.carbpol.2019.115286

15. L. Lou, R.J. Kendall, E. Smith, S.S. Ramkumar, Functional PVDF/rGO/TiO$_2$ nanofiber webs for the removal of oil from water. Polymer **186**, 122028 (2020). https://doi.org/10.1016/j.polymer.2019.122028

16. H. Meng, J. Wan, J. Jing, D. Sun, B. Jiang, F. Liang, Z. Yang, Magnetic responsive polymer nanofiber composites for easy collecting chemical spills. Chin. Chem. Lett. **31**, 253–255 (2020). https://doi.org/10.1016/j.cclet.2019.04.002

17. L. Li, L. Rong, Z. Xu, B. Wang, X. Feng, Z. Mao, H. Xu, J. Yuan, S. Liu, X. Sui, Cellulosic sponges with pH responsive wettability for efficient oil-water separation. Carbohydr. Polym. **237**, 116133 (2020). https://doi.org/10.1016/j.carbpol.2020.116133

18. M.A. Mahmoud, Oil spill cleanup by raw flax fiber: modification effect, sorption isotherm, kinetics and thermodynamics. Arab. J. Chem. **13**, 5553–5563 (2020). https://doi.org/10.1016/j.arabjc.2020.02.014

19. J. Wang, Y. Zheng, A. Wang, Investigation of acetylated kapok fibers on the sorption of oil in water. J. Environ. Sci. **25**(2), 246–253 (2013). https://doi.org/10.1016/S1001-0742(12)60031-X

20. J. Wang, Y. Zheng, Y. Kang, A. Wang, Investigation of oil sorption capability of PBMA/SiO$_2$ coated kapok fiber. Chem. Eng. J. **223**, 632–6327 (2013). https://doi.org/10.1016/j.cej.2013.03.007

21. N. Ali, M. El-Harbawi, A.A. Jabal, C.Y. Yin, Characteristics and oil sorption effectiveness of kapok fibre, sugarcane bagasse and rice husks: oil removal suitability matrix. Environ. Technol **33**(4), 481–486 (2012). https://doi.org/10.1080/09593330.2011.579185

22. A. El Nemr, S. Ragab, Acetylation of Cotton-Giza 86 cellulose using $MnCl_2$ as a new catalyst and its application to machine oil removal. Environ. Processes **5**(4), 895–905 (2018). https://doi.org/10.1007/s40710-018-0330-7

23. N. Baig, F.I. Alghunaimi, H.S. Dossary, T.A. Saleh, Superhydrophobic and superoleophilic carbon nanofiber grafted polyurethane for oil-water separation. Process Saf. Environ. Prot. **123**, 327–334 (2019). https://doi.org/10.1016/j.psep.2019.01.007

24. W. Wang, J. Lin, J. Cheng, Z. Cui, J. Si, Q. Wang, X. Peng, T.L. Sheng, Dual super-amphiphilic modified cellulose acetate nanofiber membranes with highly efficient oil/water separation and excellent antifouling properties. J. Hazard Mater. **385**, 121582 (2020). https://doi.org/10.1016/j.jhazmat.2019.121582

25. Y. Yi, H. Tu, X. Zhou, R. Liu, Y. Wu, D. Li, Q. Wang, X. Shi, H. Deng, Acrylic acid-grafted pre-plasma nanofibers for efficient removal of oil pollution from aquatic environment. J. Hazard Mater. **371**, 165–174 (2019). https://doi.org/10.1016/j.jhazmat.2019.02.085

26. H. Li, L.F. Liu, F.L. Yang, Hydrophobic modification of polyurethane foam for oil spill cleanup. Mar. Pollut. Bull. **64**(8), 1648–1653 (2012). https://doi.org/10.1016/j.marpolbul.2012.05.039

27. M.M. Alghamdi, A.A. El-Zahhar, A.M. Idris, T.O. Sadi, T. Sahlabji, A. El Nemr, Synthesis, characterization and application of a new polymeric-clay-magnetite composite resin for water softening. Sep. Purif. Technol. **224**, 356–365 (2019). https://doi.org/10.1016/j.seppur.2019.05.037

28. A. El Nemr, E. Serag, A. El-Maghraby, S.A. Fathy, F.F. Abdel Hamid, Manufacturing of pH sensitive PVA/PVP/MWCNT and PVA/PEG/MWCNT nanocomposites: an approach for significant drug release. J. Macromol. Sci. Part A **56**(8), 781–793 (2019). https://doi.org/10.1080/10601325.2019.1607377

29. J.Y. Lin, B. Ding, J.M. Yang, J.Y. Yu, G. Sun, Subtle regulation of the micro- and nano structures of electrospun polystyrene fibers and their application in oil absorption. Nanoscale **4**(1), 176–182 (2012). https://doi.org/10.1039/C1NR10895F

30. W. Chai, X. Liu, J. Zou, X. Zhanga, B. Li, T. Yin, Pomelo peel modified with acetic anhydride and styrene as new sorbents for removal of oil pollution. Carbohydr. Polym. **132**, 245–251 (2015). https://doi.org/10.1016/j.carbpol.2015.06.060

31. H.T.T. Duong, R.P. Burford, Effect of foam density, oil viscosity, and temperature on oil sorption behavior of polyurethane. J. Appl. Polym. Sci. **99**(1), 360–367 (2006). https://doi.org/10.1002/app.22426

32. N. Chen, Q.M. Pan, Versatile fabrication of ultralight magnetic foams and application for oil-water separation. ACS Nano **7**(8), 6875–6883 (2013). https://doi.org/10.1021/nn4020533

33. A. Pavía-Sanders, S. Zhang, J.A. Flores, J.E. Sanders, J.E. Raymond, K.L. Wooley, Robust magnetic/polymer hybrid nanoparticles designed for crude oil entrapment and recovery in aqueous environments. ACS Nano **7**(9), 7552–7561 (2013). https://doi.org/10.1021/nn401541e

34. L. Ding, Y. Li, D. Jia, J.P. Deng, W.T. Yang, Beta-cyclodextrin-based oil-absorbents: preparation, high oil absorbency and reusability. Carbohyd. Polym. **83**(4), 1990–1996 (2011). https://doi.org/10.1016/j.carbpol.2010.11.005

35. N. Bhardwaj, S.C. Kundu, Electrospinning: a fascinating fiber fabrication technique. Biotechnol. Adv. **28**, 325–347 (2010). https://doi.org/10.1016/j.biotechadv.2010.01.004

36. Y. Chen, L. Qiu, X. Ma, L. Dong, Z. Jin, G. Xia, P. Du, J. Xiong, Electrospun cellulose polymer nanofiber membrane with flame resistance properties for lithium-ion batteries. Carbohydr. Polym. **234**, 115907 (2020). https://doi.org/10.1016/j.carbpol.2020.115907

37. F. Liu, X. Li, L. Wang, X. Yan, D. Ma, Z. Liu, X. Liu, Sesamol incorporated cellulose acetate-zein composite nanofiber membrane: an efficient strategy to accelerate diabetic wound healing. Int. J. Biol. Macromol. **149**, 627–638 (2020). https://doi.org/10.1016/j.ijbiomac.2020.01.277

38. D.S. de Almeida, E.H. Duarte, E.M. Hashimoto, F.R.B. Turbiani, E.C. Muniz, P.R. de Souza, M.L. Gimenes, L.D. Martins, Development and characterization of electrospun cellulose acetate nanofibers modified by cationic surfactant. Polym. Test. **81**, 106206 (2020). https://doi.org/10.1016/j.polymertesting.2019.106206

39. B. Li, X. Yang, Rutin-loaded cellulose acetate/poly(ethylene oxide) fiber membrane fabricated by electrospinning: a bioactive material. Mater. Sci. Eng. C **109**, 110601 (2020). https://doi.org/10.1016/j.msec.2019.110601

40. F. Ahmed, S. Saleemi, Z. Khatri, M.I. Abro, I.-S. Kim, Co-electrospun poly(-caprolactone)/cellulose nanofibers-fabrication and characterization. Carbohydr. Polym. **115**, 388–393 (2015). https://doi.org/10.1016/j.carbpol.2014.09.002

41. D.B. Nugroho, A. Rianjanu, K. Triyana, Kusumaatmaja A and Roto R Quartz crystal microbalance-coated cellulose acetate nanofibers overlaid with chitosan for detection of acetic anhydride vapor. Results Phys. **15**, 102680 (2019). https://doi.org/10.1016/j.rinp.2019.102680

42. Y. Luo, S. Wang, M. Shen, R. Qi, Y. Fang, R. Guo, H. Cai, X. Cao, H. Tomás, M. Zhu, X. Shi, Carbon nanotube-incorporated multilayered cellulose acetate nanofibers for tissue engineering applications. Carbohydr. Polym. **91**(1), 419–427 (2013). https://doi.org/10.1016/j.carbpol.2012.08.069

43. A. Ullah, S. Ullah, M.Q. Khan, M. Hashmi, P.D. Nam, Y. Kato, Y. Tamada, I.S. Kim, Manuka honey incorporated cellulose acetate nanofibrous mats: fabrication and in vitro evaluation as a potential wound dressing. Int. J. Biol. Macromol. **155**, 479–489 (2020). https://doi.org/10.1016/j.ijbiomac.2020.03.237

44. A.R.S. Priya, A. Subramania, Y.-S. Jung, K.-J. Kim, High-performance quasi-solid-state dye-sensitized solar cell based on an electrospun PVdF_HFP membrane electrolyte. Langmuir **24**, 9816–9819 (2008). https://doi.org/10.1021/la801375s

45. A.M. Omer, R.E. Khalifa, T.M. Tamer, M. Elnouby, A.M. Hamed, Y.A. Ammar, A.A. Ali, M. Gouda, M.S. MohyEldin, Fabrication of a novel low-cost superoleophilic nonanyl chitosan-poly (butyl acrylate) grafted copolymer for the adsorptive removal of crude oil spills. Int. J. Biol. Macromol. **140**, 588–599 (2019). https://doi.org/10.1016/j.ijbiomac.2019.08.169

46. S.F. Chin, A.N.B. Romainor, S.C. Pang, Fabrication of hydrophobic and magnetic cellulose aerogel with high oil absorption capacity. Mater. Lett. **115**, 241–243 (2014). https://doi.org/10.1016/j.matlet.2013.10.061

47. Y.O. Kang, J.N. Im, W.H. Park, Morphological and permeable properties of antibacterial double-layered composite nonwovens consisting of microfibers and nanofibers. Compos. Part B Eng. **75**, 256–263 (2015). https://doi.org/10.1016/j.compositesb.2015.01.029

48. A. El Nemr, S. Ragab, A. El Sikaily, A. Khaled, Synthesis of cellulose triacetate from cotton cellulose by using NIS as a catalyst under mild reaction conditions. Carbohydr. Polym. **130**, 41–48 (2015). https://doi.org/10.1016/j.carbpol.2015.04.065

49. A. El Nemr, S. Ragab, A. El Sikaily, Testing Zinc chloride as a new catalyst for direct synthesis of cellulose di- and tri-acetate in a solvent free system under microwave irradiation. Carbohydr. Polym. **151**, 1058–1067 (2016). https://doi.org/10.1016/j.carbpol.2016.06.072

50. A. El Nemr, S. Ragab, A. El Sikaily, Rapid synthesis of cellulose triacetate from cotton cellulose and its effect on specific surface area and particle size distribution. Iran Polym. J. **26**(4), 261–272 (2017). https://doi.org/10.1007/s13726-017-0516-2

51. X. Zheng, Z. Guo, D. Tian, X. Zhang, W. Li, L. Jiang, Underwater self-cleaning scaly fabric membrane for oily water separation. ACS Appl. Mater. Interfaces **7**(7), 4336–4343 (2015). https://doi.org/10.1021/am508814g

52. Q. Ma, H. Cheng, A.G. Fane, R. Wang, H. Zhang, Recent development of advanced materials with special wettability for selective oil/water separation. Small **12**(16), 2186–2202 (2016). https://doi.org/10.1002/smll.201503685

53. S. Ragab, A. El Nemr, Nanofiber cellulose Di- and Tri-acetate using ferric chloride as a catalyst promoting highly efficient synthesis under microwave irradiation. J. Macromol. Sci. Part A Pure Appl. Chem. **55**(2), 124–134 (2018). https://doi.org/10.1080/10601325.2017.1387741

54. S. Ragab, A. El Nemr, Zirconyl chloride as a novel and efficient green Lewis acid catalyst for direct acetylation of cotton cellulose in the presence and absence of solvent. J. Polym. Res. **26**, 156 (2019). https://doi.org/10.1007/s10965-019-1816

55. H. Wu, Z.-M. Wang, A. Kumagai, T. Endo, Amphiphilic cellulose nanofiber-interwoven graphene aerogel monolith for dyes and silicon oil removal. Compos. Sci. Technol. **171**, 190–198 (2019). https://doi.org/10.1016/j.compscitech.2018.12.017

56. A. Eleryan, A. El Nemr, A. M. Idris, M. M. Alghamdi, A. A. El-Zahhar, Said TO and Sahlabji T, Feasible and eco-friendly removal of hexavalent chromium toxicant from aqueous solutions using chemically modified sugarcane bagasse cellulose. (2020) Toxin Reviews. In press 09 July, 2020. https://doi.org/10.1080/15569543.2020.1790606

57. D. Bu, X. Hu, Z. Yang, X. Yang, W. Wei, M. Jiang, Z. Zhou, A. Zaman, Elucidation of the relationship between intrinsic viscosity and molecular weight of cellulose dissolved in Tetra-N-Butyl Ammonium Hydroxide/Dimethyl Sulfoxide. Polymers **11**, 1605 (2019). https://doi.org/10.3390/polym11101605

58. M. Kostag, K. Jedvert, C. Achtel, T. Heinze, O.A. El Seoud, Recent advances in solvents for the dissolution, shaping and derivatization of cellulose: quaternary ammonium electrolytes and their solutions in water and molecular solvents. Molecules **23**, 1–38 (2018). https://doi.org/10.3390/molecules23030511

59. M.A. Hussain, T. Liebert, T. Heinze, Acylation of cellulose with N, N′-carbonyldiimidazole-activated acids in the novel solvent dimethyl sulfoxide/tetrabutylammonium fluoride. Macromol. Rapid Commun. **25**, 916–920 (2004). https://doi.org/10.1002/marc.200300308

60. L. Zhang, T.J. Menkhaus, H. Fong, Fabrication and bio separation studies of adsorptive membranes/felts made from electrospun cellulose acetate nanofibers. J. Membr. Sci. **319**, 176–184 (2008). https://doi.org/10.1016/j.memsci.2008.03.030

61. M.S. Mohy Eldin, Y.A. Ammar, T.M. Tamer, A.M. Omer, A.A. Ali, Development of low-cost chitosan derivatives based on marine waste sources as oil adsorptive materials: I. preparation and characterization. Desalin. Water Treat. **72**, 41–51 (2017). https://doi.org/10.1002/smll.201503685

62. M.S. Mohy Eldin, A.M. Omer, T.M. Tamer, M.H. Abd Elmageed, M.E. Youssef, R.E. Khalifa, Novel aminated cellulose acetate membranes for direct methanol fuel cells (DMFCs). Int. J. Electrochem. Sci. **12**, 4301–4318 (2017). https://doi.org/10.20964/2017.05.67

63. P.-C. Chen, X.-J. Huang, F. Huang, Y. Ou, M.-R. Chen, Z.-K. Xu, Immobilization of lipase onto cellulose ultrafine fiber membrane for oil hydrolysis in high performance bioreactor. Cellulose **18**, 1563–1571 (2011). https://doi.org/10.1007/s10570-011-9593-0

64. N.M. Bedford, A.J. Steck, Photocatalytic self-cleaning textile fibers by coaxial electrospinning. ACS Appl. Mater. Interfaces **2**, 2448–2455 (2010). https://doi.org/10.1021/am1005089

65. L. Shuiping, T. Lianjiang, H. Weili, L. Xiaoqiang, C. Yanmo, Cellulose acetate nanofibers with photochromic property: fabrication and characterization. Mater. Lett. **64**, 2427–2430 (2010). https://doi.org/10.1016/j.matlet.2010.08.018

66. R.E. Ghonim, A.M. Omer, T.M. Tamer, W. Salem, M.S. Mohyeldin, Removal of methylene blue dye from synthetic aqueous solutions using novel phosphonate cellulose acetate membranes: adsorption kinetic, equilibrium, and thermodynamic studies. Desalin. Water Treat. **144**, 272–285 (2019). https://doi.org/10.5004/dwt.2019.23323

67. N.K.R. Konwarh, M. Misra, Electrospun cellulose acetatenanofibers: the present status and gamut of biotechnological applications. Biotechnol. Adv. **31**, 421–437 (2013). https://doi.org/10.1016/j.biotechadv.2013.01.002

68. T. Lan, Z.-Q. Shao, M.-J. Gu, Z.-W. Zhou, Y.-l Wang, W.-J. Wang, F.-J. Wang, J.-Q. Wang, Electrospun nanofibrous cellulose diacetate nitrate membrane for protein separation. J. Membr. Sci. **489**, 204–211 (2015). https://doi.org/10.1016/j.memsci.2015.04.009

69. C. Ao, W. Yuan, J. Zhao, X. He, X. Zhang, Q. Li, T. Xia, W. Zhang, C. Lu, Super hydrophilic graphene oxide @electrospun cellulose nanofiber hybrid membrane for high-efficiency oil/water separation. Carbohydr. Polym. **175**(1), 216–222 (2017). https://doi.org/10.1016/j.carbpol.2017.07.085

70. O. Arslan, Z. Aytac, T. Uyar, Superhydrophobic, hybrid, electrospun cellulose acetate nanofibrous mats for oil/water separation by tailored surface modification. ACS Appl. Mater. Interfaces **8**, 19747–19754 (2016). https://doi.org/10.1021/acsami.6b05429

71. F. Sun, W. Liu, Z. Dong, Y. Deng, Underwater superoleophobicity cellulose nanofibril aerogel through regioselective sulfonation for oil/water separation. Chem. Eng. J. **330**, 774–782 (2017). https://doi.org/10.1016/j.cej.2017.07.142

72. M. Voll, P. Kleinschmit, Carbon. In: Ullmann's Encyclopedia of Industrial Chemistry, Wiley, New York (2002). https://doi.org/10.1002/14356007

73. H. Kato, A. Nakamura, M. Horie, S. Endoh, K. Fujita, H. Iwahashi, S. Kinugasa, Preparation and characterization of stable dispersions of carbon black and nano-diamond in culture medium for in vitro toxicity assessment. Carbon **49**, 3989–3997 (2011). https://doi.org/10.1016/j.carbon.2011.05.039

74. J.F. Auchter, *Chemical Economics Handbook: Carbon Black* (Menlo Park, CA, SRI Consulting, 2005)

75. A. Celebioglu, T. Uyar, Electrospun porous cellulose acetate fibers from volatile solvent mixture. Mater. Lett. **65**, 2291–2294 (2011). https://doi.org/10.1016/j.matlet.2011.04.039

76. S. De Vrieze, T. Van Camp, A. Nelvig, B. Hagström, P. Westbroek, K. De Clerck, The effect of temperature and humidity on electrospinning. J. Mater. Sci. **44**, 1357–1362 (2009). https://doi.org/10.1007/s10853-008-3010-6

77. S. Hernández-López, E. Vigueras-Santiago, M.M. Mora, J.R.F. Mancilla, E.A.Z. Contreras, Cellulose-based polymer composite with carbon black for tetrahydrofuran sensing. Int. J. Polym. Sci. (2013). https://doi.org/10.1155/2013/381653

78. G. Salihu, P. Goswami, S. Russell, Hybrid electrospun nonwovens from chitosan/cellulose acetate. Cellulose **19**, 739–749 (2012). https://doi.org/10.1007/s10570-012-9666-8

79. T.M. Eldeeb, A. El Nemr, M.H. Khedr, S.I. El-Dek, N.G. Imam, Novel, three-dimensionoal, chitosan-carbon nanotube–PVA nanocomposite hydrogel for removal of Cr^{6+} from water. Desalin. Water Treat. **184**, 163–177 (2020). https://doi.org/10.5004/dwt.2020.25366

80. E. Serag, A. El Nemr, S.A. Fathy, F.F. Abdel Hamid, A. El-Maghraby, A novel three dimensional Carbon Nanotube-polyethylene glycol-Polyvinyl alcohol Nanocomposite for Cu (II) removal from water. Egypt J. Aquat. Biol. Fish. **22**(2), 103–118 (2018). https://doi.org/10.21608/ejabf.2018.8234

81. M. Likon, M. Remškar, V. Ducman, F. Šveg, Populus seed fibers as a natural source for production of oil super absorbents. J. Environ. Manag. **114**, 158–167 (2013). https://doi.org/10.1016/j.jenvman.2012.03.047

82. T.-T. Lim, X. Huang, Evaluation of kapok (Ceibapentandra (L) Gaertn) as a natural hollow hydrophobic–oleophilic fibrous sorbent for oil spill cleanup. Chemosphere **66**, 955–963 (2007). https://doi.org/10.1016/j.chemosphere.2006.05.062

83. ASTM (1993) Annual Book of American Society for Testing and Materials (ASTM) Standard section, Standard method of test for water and sediment in crude oil and fuel oils by centrifuge, D1796–91, 17, Philadelphia, PA., 1993

84. G. Alaa El-Din, A. Amer, G. Malsh, M. Hussein, Study on the use of banana peels for oil spill removal. Alexandria Eng. J **57**, 2061–2068 (2018). https://doi.org/10.1016/j.aej.2017.05.020

85. A. El Nemr, A. El-Sikaily, A. Khaled, Modeling of adsorption isotherms of methylene blue onto rice husk activated carbon. Egypt J. Aquat. Res. **36**(3), 403–425 (2010). https://doi.org/10.1016/j.scitotenv.2020.138325

86. M.A. Hassaan, A. El Nemr, F.F. Madkour, Advanced oxidation processes of mordant violet 40 dye in freshwater and seawater. Egypt J. Aquat. Res. **43**, 1–9 (2017). https://doi.org/10.1016/j.ejar.2016.09.004

87. M.A. Hassaan, A. El Nemr, F.F. Madkour, Testing the advanced oxidation processes on the degradation of direct blue 86 dye in wastewater. Egypt J. Aquat. Res. **43**, 11–19 (2017). https://doi.org/10.1016/j.ejar.2016.09.006

88. C. Chen, L. Wang, Y. Huang, Crosslinking of the electrospun polyethylene glycol/cellulose acetate composite fibers as shape-stabilized phase change materials. Mater. Lett. **63**, 569–571 (2009). https://doi.org/10.1016/j.matlet.2008.11.033

89. M.S. Mohy Eldin, M.H. Abd Elmageed, A.M. Omer, T.M. Tamer, M.E. Yossuf, R.E. Khalifa, Development of novel phosphorylated cellulose acetate polyelectrolyte membranes for direct methanol fuel cell application. Int. J. Electrochem. Sci. **11**, 3467–3491 (2016). https://doi.org/10.20964/110318

90. S.J. Gregg, *Sing KSW Adsorption, Surface Area and Porosity*, 2nd edn. (Academic Press, London, 1982)

91. K.S.W. Sing, D.H. Everett, R.A.W. Haul, L. Moscou, R.A. Pierotti, J. Rouquerol, T. Siemieniewska, Reporting Physisorption data for gas/solid interface with special reference to the determination of surface area and porosity. Pure Appl Chem. **57**, 603–619 (1985). https://doi.org/10.1351/pac198557040603

92. L.A. Goetz, B. Jalvo, R. Rosal, A.P. Mathew, Super hydrophilic-canti- fouling electrospun cellulose acetate membranes coated with chitin nanocrystals for water filtration. J. Membrane Sci. **510**, 238–248 (2016). https://doi.org/10.1016/j.memsci.2016.02.069

93. A. El Nemr, A. Eleryan, M. Mashaly, A. Khaled, Comparative study of synthesis of cellulose propionate from different sources using NIS as a new catalyst. Polym. Bull. **78**, 4369–4386 (2020). https://doi.org/10.1007/s00289-020-03313-1

94. A. El Nemr, A. Eleryan, M. Mashaly, A. Khaled, Rapid synthesis of cellulose propionate and its conversion to cellulose nitrate propionate. Polym. Bull. **78**, 4149–4182 (2020). https://doi.org/10.1007/s00289-020-03317-x

95. T.M. Eldeeb, A. El Nemr, M.H. Khedr, S.I. El-Dek, Novel bio-nanocomposite for efficient copper removal. Egypt J. Aquat. Res. **47**, 261–267 (2021). https://doi.org/10.1016/j.ejar.2021.07.002

96. X. Shi, Y. Zheng, G. Wang, Q. Lin, J. Fan, pH and electro-response characteristics of bacterial cellulose nanofiber/sodium alginate hybrid hydrogels for dual controlled drug delivery. RSC Adv. **4**, 47056–47065 (2014). https://doi.org/10.1039/C4RA09640A

97. J. Bhandari, H. Mishra, P.K. Mishra, R. Wimmer, F.J. Ahmad, S. Talegaonkar, Cellulose nanofiber aerogel as a promising biomaterial for customized oral drug delivery. Int. J. Nanomed. **12**, 2021–2031 (2017). https://doi.org/10.2147/IJN.S124318

98. M. Abdullah, A.U. Rahmah, Z. Man, Physicochemical and sorption characteristics of Malaysian Ceibapentandra (L) Gaertn as a natural oil sorbent. J. Hazard Mater. **177**, 683–691 (2010). https://doi.org/10.1016/j.jhazmat.2009.12.085

99. T. Dong, G. Xu, F. Wang, Oil spill cleanup by structured natural sorbents made from cattail fibers. Ind. Crops Prod. **76**, 25–33 (2015). https://doi.org/10.1016/j.indcrop.2015.06.034

100. N.E. Thompson, G.C. Emmanue, K.J. Adagadzu, N.B. Yusuf, Sorption studies of crude oil on acetylated rice husks. Arch. Appl. Sci. Res. **2**(5), 142–151 (2010)

101. M.D. Teli, S.P. Valia, Acetylation of banana fiber to improve oil absorbency. Carbohydr. Polym. **92**, 328–333 (2013). https://doi.org/10.1016/j.carbpol.2012.09.019